Received: October 10, 2024. Revised: October 31, 2024. 268

International Journal of
Intelligent Engineering & Systems

http://www.inass.org/

# Short-Term Peak Load Forecasting Using Interval Type-2 Fuzzy Logic - Horse Herd Optimization Algorithm in Sulbagsel Electricity System

**Syafaruddin[1]* Imam Robandi[2] Rini Nur Hasanah[3] Yusri Syam Akil[1]**
**Harus Laksana Guntur[4] Vita Lystianingrum[2] Muhammad Ruswandi Djalal[2]**
**Mohamad Almas Prakasa[2]**

*[1]Department of Electrical Engineering, Universitas Hasanuddin, Indonesia*
*[2]Departement of Electrical Engineering, Institut Teknologi Sepuluh Nopember, Indonesia*
*[3]Departement of Electrical Engineering, Universitas Brawijaya, Indonesia*
*[4]Departement of Mechanical Engineering, Institut Teknologi Sepuluh Nopember, Indonesia*
* Corresponding author's Email: syafaruddin@unhas.ac.id

**Abstract:** This paper discusses short-term peak load forecasting for the South Sulawesi system (Sulbagsel), Indonesia. The peak load is forecasted using interval type-2 fuzzy logic (IT2FL) combined with the horse herd optimization algorithm (HHOA). The HHOA method is employed to optimize the footprint of uncertainty (FOU) in fuzzy logic, including both the antecedent (X, Y) and the consequent (Z). This approach is applied using daily peak load data from the four days prior to the forecasted day (d-4) and the forecasted day itself (d). To compare the HHOA method, similar swarm intelligence techniques, the cuckoo search algorithm (CSA) and Bat Algorithm (BA), are also used. The test results show that IT2FL-HHOA provides more accurate forecasting, as indicated by a significantly lower mean absolute percentage error (MAPE). The MAPE for IT2FL-HHOA is 1.5567%, while for IT2FL-CSA, it is 1.6289%, and for IT2FL-BA, it is 1.6386%. For the Type-1 fuzzy logic (IT1FL-HHOA) method, the MAPE is 1.6604%, for IT1FL-CSA it is 1.6730%, and for IT1FL-BA it is 1.6704%.

**Keywords:** Short-term, Load forecasting, Sulbagsel electricity system, HHOA, MAPE.

## 1. Introduction

Short-term load forecasting (STLF) is a tool designed to predict load demand with lead times ranging from a few hours to a week. The insights provided by STLF facilitate accurate decision-making regarding load management, pumped storage scheduling, unit commitment, and load dispatch [1]. This enables electric utilities to optimize steady-state operations safely, enhancing reliability and reducing operating costs. However, inaccurate load estimates can lead to suboptimal reserve utilization, adversely impacting operating expenses [2]. If load demand is not accurately predicted, it may become necessary to purchase costly peaking units, potentially resulting in grid overload or significant failures. Conversely, overestimating demand can lead to unnecessary increases in reserves, driving up operating costs [2].

In recent decades, substantial progress has been made in various STLF techniques, evolving from manual methods to advanced computerized models [3]. STLF techniques can be categorized into two main types: conventional and modern. Conventional techniques encompass statistical models that utilize historical data and specific events, such as holidays or celebrations, to perform hourly or weekly load forecasts [4].

Statistical approaches are typically offline forecasting techniques that utilize time functions and demonstrate effectiveness in estimating linear curves. However, because load forecasting is inherently non-linear, these methods often yield less accurate results compared to modern techniques [5]. The uncertainty and increasing complexity of contemporary loads have led to greater forecasting errors with traditional methods. Contributing factors to these errors include

weather conditions, seasonal variations, shifts among customer classes, and climate change, all of which contribute to the dynamic nature of load performance.

Feasible solutions that often demonstrate promising features can be efficiently obtained using artificial intelligence (AI) techniques, such as fuzzy logic, artificial neural networks (ANN), and evolutionary algorithms (EA). These methods have shown the capability to learn complex non-linear relationships that are challenging to model, making them appealing and widely used options for load forecasting. Swarm intelligence (SI), a branch of AI, focuses on the collective and decentralized behavior of individuals interacting with one another and their environment. Various swarm intelligence methods applied to load forecasting include particle swarm optimization (PSO) [6], bat algorithm (BA) [7], firefly algorithm (FA) [8], cuckoo search algorithm (CSA) [9], grey wolf optimization (GWO) [10], salp swarm algorithm (SWA) [11], and crow search algorithm (CrSA) [12].

In the classical AI method based on interval type-1 fuzzy logic (IT1FL), mathematical calculations derived from set theory are used to represent ambiguity through linguistic variables. IT1FL is frequently employed in STLF [13]. However, a significant challenge with IT1FL is the form of its membership function (MF). Researchers argue that the crisp membership values of IT1FL render it inadequate for handling high levels of uncertainty. To address this issue, Zadeh introduced a concept known as type-2 fuzzy logic (IT2FL) interval sets [14], which generalize the interval sets of IT1FL. Essentially, IT2FL sets enable the handling of both linguistic and numerical uncertainties. Karnik and Mendel [15] introduced an IT2FL system that incorporates rules to address the uncertainties associated with its MF.

The application of IT2FL to forecasting problems demonstrates good performance. In the study referenced in [16], very STLF was discussed in relation to the Java-Bali system. The study in [17] explored wind power interval prediction (WPIP) as a method to support power system planning and scheduling using IT2FL. Findings from study [18] indicated that IT2FL performs effectively, producing load estimates that closely align with the target values.

The footprint of uncertainty (FOU) is crucial in characterizing IT2FL [19]. The representation of FOU is a key issue in IT2FL theory. FOU can be uniquely determined by the corresponding upper membership function (UMF) and lower membership function (LMF). Thus, the study of IT2FL often involves examining the corresponding LMF and UMF, with both being represented as IT1FL sets within the same IT2FL universe [20]. Although the FOU of an IT2FL can be specified by its corresponding LMF and UMF, its representation cannot be directly expressed in terms of the UMF and LMF. To accurately represent the FOU of a general IT2FL, the principal membership levels must be defined first.

A novel SI approach known as the horse herd optimization algorithm (HHOA) was recently introduced by Farid MiarNaeimi [21]. This algorithm draws inspiration from the social dynamics of horses across various age groups and integrates six essential characteristics: grazing, social hierarchy, sociability, imitation, protective behaviors, and roaming. HHOA is recognized as a rapid and resilient optimization algorithm [22, 23] and has been investigated for applications in power system optimization. In study [24], the implementation of HHOA was discussed as a means to enhance energy management in optimizing intelligent electric vehicle charging. Study [25] explores the application of HHOA for optimizing the performance of a solar water pump system. Additionally, this study examines maximum power extraction from a solar power system using an HHOA-based maximum power point tracking (MPPT) technique under various weather conditions [26]. In study [27], HHOA was employed for tuning PID controllers in brushless DC motor speed control. The application of HHOA in power system optimization has developed rapidly and yielded significant results. This serves as the primary motivation for the author to propose combining the HHOA method with IT2FL to optimize the FOU in IT2FL.

One of the electricity systems in Indonesia, the South Sulawesi system (Sulbagsel), exhibits complex load characteristics [28, 29] that vary significantly due to seasonal influences and community behavior. Load forecasting is crucial as it estimates electricity consumption over a specific period. Accurate forecasting of electricity loads enhances the safety and reliability of electric power system operations, including load flow management, unit maintenance, and unit commitments. This serves as the second motivation for the author to investigate the peak load forecasting problem in the Sulbagsel system.

The main contributions of this research are:

1) Applying the HHOA method to optimize the FOU MF of IT2FL in STLF for the Sulbagsel electricity system
2) Testing and validating the IT2FL-HHOA method for STLF in the Sulbagsel electricity system.

The organization of this paper is as follows: Section II provides an overview of IT2FL; Section III

outlines the research method; Section IV presents the results; and Section V concludes the study.

## 2. Interval type-2 fuzzy logic (IT2FL)

### 2.1 Interval type-2 fuzzy logic

An IT2FL, denoted as $\tilde{A}$, has a MF $\mu\tilde{A}$, where $x \in X$ and $u \in Jx \subseteq [0,1]$. Its characteristics can be identified by Eq. (1).

$$\tilde{A} = \int_{x\in X}^{x} \int_{x\in J_X}^{x} \frac{\pi\tilde{A}(x,u)}{(x,u)} Jx \subseteq [0.1] \quad (1)$$

$x$ is the primary variable with domain $X$, while $u \in U$ is a secondary variable with domain $Jx$ for each $x \in X$. $Jx$ referred to as the primary MF of $x$. The uncertainty in $\tilde{A}$ is represented by the collection of all primary MF $(Jx)$, known as the FOU of $\tilde{A}$, as shown in Eq. (2).

$$FOU(\tilde{A}) = \cup_{\forall x\in X} Jx = \{(x,u); u \in Jx \subseteq [0.1]\} \quad (2)$$

Given, $Jx$ is the interval set,

$$Jx = \left\{(x,u); u \in \left[\underline{\mu}_{\tilde{A}}(x), \bar{\mu}_{\tilde{A}}(x)\right]\right\} \quad (3)$$

Eq. (3) $FOU(\tilde{A})$ can be written as Eq. (4).

$$FOU(\tilde{A}) = \cup_{\forall x\in X} \left[\underline{\mu}_{\tilde{A}}(x), \bar{\mu}_{\tilde{A}}(x)\right] \quad (4)$$

$Jx$ is the primary MF of $x$, while $\underline{\mu}\tilde{A}$ and $\bar{\mu}\tilde{A}$ represent the LMF of $\tilde{A}$ and the UMF of $\tilde{A}$, respectively.

### 2.2 IT2FL system structure

The structure of the IT2FL, shown in Fig. 2, illustrates the IT2FL process, which maps the input values of the crisp set $x$ to output values expressed by the equation $Y=f(x)$.

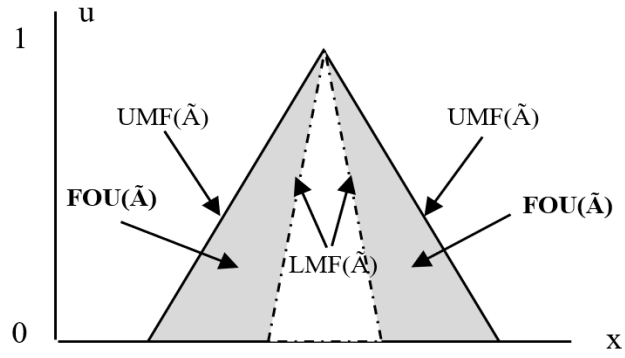


Figure. 1 IT2FL MF

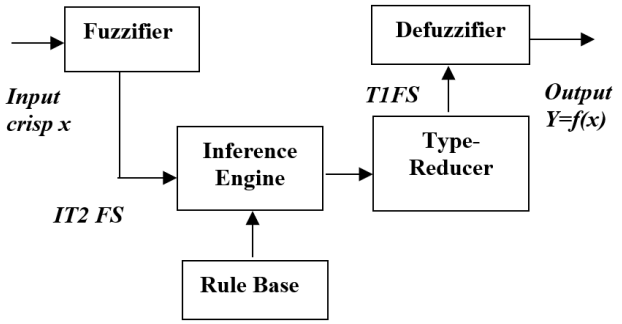


Figure. 2 IT2FL Structure

## 3. Research method

This section outlines the formulation of the proposed method and the objective function applied.

### 3.1 Horse herd optimization algorithm (HHOA)

HHOA mimics the behavior of horse herds of different ages, categorizing their behavior into six general types: Grazing, Hierarchy, Sociability, Imitation, Defense Mechanism, and Roaming [21]. Eq. (5) is used to update the positions and speeds of the horses. In this context, *Age* is represented as $\alpha$, $\beta$, $\gamma$, and $\delta$.

$$X_i^{Iter,Age} = V_i^{Iter,Age} + X_I^{(Iter-1),Age} \quad (5)$$

Where, signifies the position of the $k$ th horse, *Age* and $\bar{V}_k^{Age,Iter}$ denote the age range and velocity vector of the horse in question, respectively, with *Iter* indicating the current iteration.

In the model, $X_i^{Iter,Age}$ indicates the position of the $i$-th horse, while $V_i^{Iter,Age}$ signifies its velocity vector, with Age representing the horse's age category. The horses are classified into four age groups: Alpha (α), Beta (β), Gamma (γ), and Delta (δ). The classification is defined as follows: Delta for horses aged 0 to 5 years, Gamma for those aged 5 to 10 years, Beta for horses aged 10 to 15 years, and Alpha for horses older than 15 years. In each iteration, a detailed response matrix must be created to determine the age category of the horses. This matrix is then organized based on the relevant responses. The top 10% of the sorted matrix are categorized as Alpha horses, the next 20% as Beta horses, while approximately 30% of the remaining horses are allocated to Gamma and 40% to Delta. The velocity vector is calculated by mathematically simulating the six behaviors of the horses.

Eq. (6) represents a motion vector in the HHOA, integrating the behavioral patterns of horses across the various age groups as outlined above.

$$\begin{gathered} V_i^{Iter,\alpha} = G_i^{Iter,\alpha} + D_i^{Iter,\alpha} \\ V_i^{Itr,\alpha} = G_i^{Itr,\beta} + H_i^{Itr,\beta} + S_i^{Itr,\beta} + D_i^{Itr,\beta} \\ V_i^{Itr,\alpha} = G_i^{Itr,\beta} + H_i^{Itr,\gamma} + S_i^{Itr,\gamma} + I_i^{Itr,\gamma} \\ + D_i^{Itr,\gamma} + R_i^{Itr,\gamma} \\ V_i^{Itr,\alpha} = G_i^{Itr,\delta} + I_i^{Itr,\delta} + R_i^{Itr,\delta} \end{gathered} \tag{6}$$

#### 3.1.1. Grazing (G)

One of the most prevalent behaviors in horses is grazing, which can occur at any age during their lifespan. Eqs. (7) and (8) establish the mathematical framework for modeling this behavior. In this context, *Age* is represented as $\alpha$, $\beta$, $\gamma$, and $\delta$.

$$G_i^{Iter,Age} = g_{iter}(\breve{u} + p\breve{l})\left[X_i^{(Iter-1)}\right] \tag{7}$$

$$g_i^{Iter,Age} = g_i^{(iter-1),Age} x \omega_g \tag{8}$$

Here, $G_i^{Iter,Age}$ represents the movement of the $i_{th}$ horse, reflecting its tendency to graze.

#### 3.1.2. Hierarchy (H)

In the wild, horses gather in herds for protection against predators, exhibiting hierarchical behaviors, often with an adult stallion serving as the leader. The parameter *h* represents the tendency of all horses in the herd to follow the strongest and oldest horse. This hierarchical behavior is particularly evident in horses aged between 5 and 15 years, as described in Eqs. (9) and (10). In this context, *Age* is represented as $\alpha$, $\beta$, and $\gamma$.

$$H_i^{Itr,Age} = h_i^{Itr,Age}\left[X_*^{(Itr-1)} - X_i^{(Itr-1)}\right] \tag{9}$$

$$h_i^{Itr,Age} = h_i^{(Itr-1),Age} x \omega_h \tag{10}$$

Here, $H_k^{Age,Itr}$ denotes the position of the best horse, while $X_*^{(Itr-1)}$ illustrates the influence of the best horse's position on the velocity vector.

#### 3.1.3. Imitation (I)

Horses are social animals that can learn behaviors, such as identifying good grazing areas, by observing other horses. This behavior is particularly prevalent among younger horses and can be represented by Eqs. (11) and (12). In this context, *Age* is represented as $\gamma$.

$$I_i^{Iter,Age} = i_i^{Iter,Age}\left[\left(\frac{1}{pN}\sum_{j=1}^{pN}\hat{X}_j^{(Iter-1)}\right) - X^{(Iter-1)}\right] \tag{11}$$

$$i_i^{Iter,Age} = i_i^{(iter-1),Age} x \omega_i \tag{12}$$

Here, $I_i^{Iter,Age}$ indicates the movement vector of horse i toward the average position of the best horses located at *X*. The variable *pN* represents the number of horses at the optimal location, with a recommendation that 10% of the horses be designated as *p*.

#### 3.1.4. Sociability (S)

For social mammals, group behavior is essential for survival. Because horses are preyed upon by various predators, living in groups enhances their safety. The survival rate is higher in group living, as the collective presence allows them to evade threats more effectively. The sociability of horses can be described by Eqs. (13) and (14). In this context, *Age* is represented as $\beta$ and $\gamma$.

$$S_i^{Iter,Age} = s_i^{Iter,Age}\left[\left(\frac{1}{N}\sum_{j=1}^{N}X_j^{(Iter-1)}\right) - X_i^{(Iter-1)}\right] \tag{13}$$

$$S_i^{Iter,Age} = s_i^{(Iter-1),Age} x \omega_s \tag{14}$$

In this context, $S_i^{Iter,Age}$ epresents the social movement vector of horse *i*, which decreases by a factor of $\omega_s$ with each iteration. Additionally, *N* denotes the total number of horses. The trait of friendliness is more pronounced in the Beta (β) and Gamma (γ) age groups.

#### 3.1.5. Defense mechanism (D)

In response to perceived threats or danger, horses primarily rely on running as their defense mechanism, with fighting serving as a secondary option. Horses instinctively flee from danger, avoiding inappropriate and suboptimal responses. This defense mechanism is represented by their inclination to move away from unsuitable positions, as illustrated in Eqs. (15) and (16), which incorporate negative coefficients.

$$D_i^{Itr,Age} = -d_i^{Itr,Age}\left[\left(\frac{1}{qN}\sum_{j=1}^{qN}\hat{X}_j^{(Itr-1)}\right) - X^{(Itr-1)}\right] \quad (15)$$

$$d_i^{Itr,Age} = d_i^{(Itr-1),Age} x \omega_d \quad (16)$$

$D_i^{Itr,Age}$ represents the escape vector for the $i_{th}$ horse, calculated based on the average of the worst positions represented by the vector *X*. Additionally, *qN* signifies the horse in the worst possible position, with the assumption that *q* accounts for 20% of the total number of horses. In this context, *Age* is represented as $\alpha$, $\beta$, and $\gamma$.

#### 3.1.6. Roam (R)

Horses are very curious animals and often wander in search of new pastures and to explore their surroundings. The factor *r* is used to simulate this behavior as random movement. Young horses, in particular, tend to wander, but this behavior gradually diminishes as they mature. Wandering is described by Eqs. (17) and (18), which represent $R_i^{Iter,Age}$ as a random velocity vector for local search and avoidance of local minima. In this context, *Age* is represented as $\gamma$ and $\delta$.

$$R_i^{Iter,Age} = r_i^{Iter,Age} pX^{(Iter-1)} \quad (17)$$

$$r_i^{Iter,Age} = r_i^{(Iter-1),Age} x \omega_r \quad (18)$$

### 3.2 Objective function

#### 3.2.1. Pre-processing

The pre-processing stage involves collecting daily electricity load data from 2010 to 2016, then grouping the data for the electricity load on each January 4th during this period.

#### 3.2.2. Processing

The processing stage involves modeling STLF using the proposed IT2FL-HHOA method, which is described as follows:

1) Create an IT2FL input MF, referred to as input *X*, and an output MF, referred to as Z, for the day to be forecasted, with the following provisions:
   X1-X6 : Load data for the years 2010-2015.
   Z1 : Forecast of the predicted day
2) Optimize the MF of the IT2FL, specifically the antecedents (X1, X2, X3, X4, X5, X6) and the consequent (Z), using the HHOA to achieve the best value for the FOU.
3) Create IT2FL fuzzy rules as follows:
   IF X is $A_i$ AND Y is $B_i$ THEN Z is $C_i$
4) Applying AND operation on IT2FL
5) Applying the MIN implication function to rules

Apply the MAX implication composition to rules

#### 3.2.3. Post-processing

Next, calculate the mean absolute percentage error (MAPE) for STLF using Eq. (19).

$$MAPE\% = \left|\frac{P_{forecast} - P_{actual}}{P_{actual}}\right| x100 \quad (19)$$

The MAPE value is compared with the load forecasting errors obtained using the IT1FL-CSA, IT1FL-BA, IT1FL-HHOA, IT2FL-CSA, IT2FL-BA, and IT2FL-HHOA methods.

### 3.3 Load data profile

This study focuses on the Sulbagsel electricity system in Indonesia, which connects major load centers across the provinces of South, Southeast, and West Sulawesi [30, 31]. For forecasting, 24-hour load data from January 4, 2016, was utilized. Consequently, load data from January 4, 2010, to 2015, was grouped as input data for the fuzzy logic model. The following section presents the results of the load data grouping for January 4, 2010, to 2015.

### 3.4 Fuzzy logic design

In accordance with the load data profile shown in Fig. 3, the next step is to design the input for both IT1FL and IT2FL using six inputs, consisting of load data from the same date over the past six years (2010

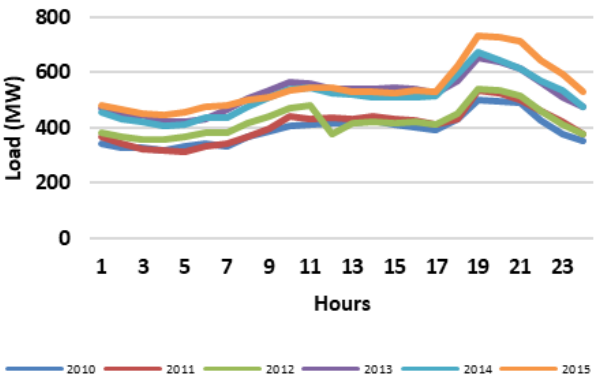


Figure. 3 Electrical load profile January 4, 2010-2015

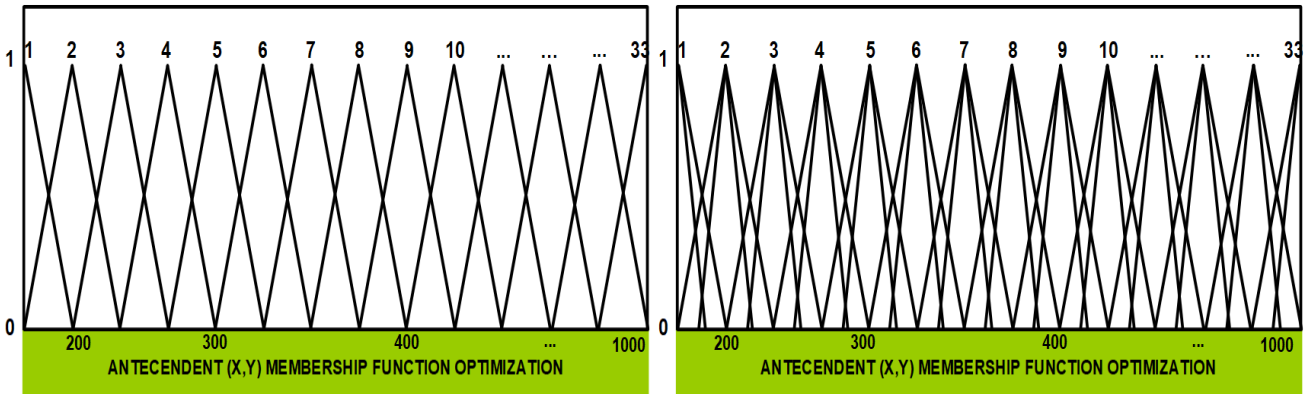


(a) (b)

Figure. 4: (a) X,Y,Z IT1FL input design and (b) X,Y,Z IT2FL input design

to 2015). Fig. 4(a) illustrates the design for IT1FL, while Fig, 4(b) shows the design for IT2FL.

### 3.5 Membership function (MF) design

The MF design for both IT1FL and IT2FL utilizes 33 fuzzy sets, each covering a range of 200 to 1000 MW. The design of the MF is presented in Table 1.

Table 2 presents the results of the fuzzy logic rules for load forecasting on January 4, 2016. Here, X1 represents the load data from 2010, X2 from 2011, X3 from 2012, X4 from 2013, X5 from 2014, X6 from 2015, and Z represents the output. For Z (output), an average range between 15 and 19 was chosen based on the load data.

Table 1. Load grouping

| Group | Load (MW) | Group | Load (MW) |
|---|---|---|---|
| 1 | [200 225] | 17 | [600-625] |
| 2 | [225 250] | 18 | [625 650] |
| 3 | [250 275] | 19 | [650 675] |
| 4 | [275 300] | 20 | [675 700] |
| 5 | [300 325] | 21 | [700 725] |
| 6 | [325 350] | 22 | [725 750] |
| 7 | [350 375] | 23 | [750 775] |
| 8 | [375 400] | 24 | [775 800] |
| 9 | [400 425] | 25 | [800 825] |
| 10 | [425 450] | 26 | [825 850] |
| 11 | [450 475] | 27 | [850 875] |
| 12 | [475 500] | 28 | [875 900] |
| 13 | [500 525] | 29 | [900 925] |
| 14 | [525 550] | 30 | [925 950] |
| 15 | [550 575] | 31 | [950 975] |
| 16 | [575 600] | 32 | [975 1000] |
| | | 33 | [1000 1025] |

Table 2. Fuzzy rules load forecasting January 4, 2016

| No | X1 | X2 | X3 | X4 | X5 | X6 | Z |
|---|---|---|---|---|---|---|---|
| 1 | 6 | 7 | 8 | 11 | 11 | 9 | 15 |
| 2 | 6 | 7 | 8 | 11 | 11 | 10 | 16 |
| 3 | 6 | 7 | 8 | 11 | 11 | 11 | 17 |
| 4 | 6 | 7 | 8 | 11 | 11 | 12 | 18 |
| 5 | 6 | 7 | 8 | 11 | 11 | 13 | 19 |
| 6 | 6 | 6 | 7 | 10 | 10 | 10 | 15 |
| 7 | 6 | 6 | 7 | 10 | 10 | 11 | 16 |
| 8 | 6 | 6 | 7 | 10 | 10 | 12 | 17 |
| 9 | 6 | 6 | 7 | 10 | 10 | 13 | 18 |
| 10 | 6 | 6 | 7 | 10 | 10 | 14 | 19 |
| 11 | 6 | 5 | 7 | 10 | 9 | 10 | 15 |
| 12 | 6 | 5 | 7 | 10 | 9 | 11 | 16 |
| 13 | 6 | 5 | 7 | 10 | 9 | 12 | 17 |
| 14 | 6 | 5 | 7 | 10 | 9 | 13 | 18 |
| 15 | 6 | 5 | 7 | 10 | 9 | 14 | 19 |
| . | . | . | . | . | . | . | . |
| . | . | . | . | . | . | . | . |
| - | - | - | - | - | - | - | - |
| 106 | 6 | 7 | 8 | 11 | 12 | 10 | 16 |
| 107 | 6 | 7 | 8 | 11 | 12 | 11 | 17 |
| 108 | 6 | 7 | 8 | 11 | 12 | 12 | 18 |
| 109 | 6 | 7 | 8 | 11 | 12 | 13 | 19 |
| 110 | 6 | 7 | 8 | 11 | 12 | 14 | 20 |

## 4. Results and discussion

This section discusses the application of the HHOA method for optimizing STLF in the Sulbagsel system. A case study focusing on the peak load in the Sulbagsel system is used to test the effectiveness of the HHOA method.

### 4.1 Benchmarking analysis

Before implementing the HHOA method for optimization, a benchmark analysis was conducted using the CSA and BA methods for comparison. This analysis aimed to evaluate the exploration and

exploitation capabilities of each method. The algorithm parameters are outlined in Table 3.

Six benchmark test functions, consisting of both unimodal and multimodal types, are presented in Table 4. The unimodal functions are used to evaluate the algorithm's exploitation ability, while the multimodal functions assess its exploration capability. This dual approach provides a comprehensive evaluation of the algorithms' performance across different optimization challenges. The fixed-dimension multimodal functions specifically test the algorithm's ability to handle low-dimensional optimization cases. The HHOA was executed 30 times, and the results, including the best values and standard deviations, are shown in Table 5.

Table 3. Parameter of the algorithms.

| Algorithm | Parameter | Value |
|---|---|---|
| CSA | Population size | 25 |
| | Dim of the problem | 15 |
| | Discovery rate | 0.25 |
| BA | Bat numbers | 25 |
| | Max, Min frequency | 2; 0; |
| | Loudness | 0.5 |
| | Emission rate | 0.5 |
| HHOA | Number of horses | 35 |
| | Max iteration | 100 |
| | Problem dimension | No.of genes |
| | Search domain | 15 |
| | No. Repetition of runs | 30 |
| | α, β | 0.99; 0.01 |

Table 4. Benchmark test function.

| Test Function | Range |
|---|---|
| **Unimodal Functions** | |
| $f_1(x) = \sum_{i=1}^{D} x_i^2$ | -100, 100 |
| $f_2(x) = max_i\{\|x_i\|, 1 \le i \le D\}$ | |
| $f_3(x) = \sum_{i=1}^{D} (x_i + 0.5)^2$ | |
| **Multimodal Functions** | |
| $f_4(x) = \sum_{i=1}^{n} -x_i \sin\left(\sqrt{\|x_i\|}\right)$ | -500, 500 |
| $f_5(x) = \frac{1}{4000}\sum_{i=1}^{n} x_i^2 - \prod_{i=1}^{n} \cos\left(\frac{x_i}{\sqrt{i}}\right) + 1$ | -600, 600 |
| $f_6(x) = 0.1\{sin^2(3\pi x_1) + \sum_{i=1}^{n}(x_i - 1)^2 [1 + sin^2(3\pi x_1 + 1)] + (x_n - 1)^2 [1 + sin^2(2\pi x_n)]\} + \sum_{i=1}^{n} u(x_i, 5, 100, 4)$ | -50, 50 |

Table 5. Benchmarking test results of the algorithms.

| $f$ | Statistical Parameter | Algorithm | | |
|---|---|---|---|---|
| | | CSA | BA | HHOA |
| $f_1$ | Best | 2.40E-28 | 6.02E-06 | 4.07E-32 |
| | Std. | 5.37E+03 | 6.29E-02 | 1.74E-01 |
| $f_2$ | Best | 1.69E-07 | 7.29E-02 | 5.67E-12 |
| | Std. | 5.44E+00 | 2.11E-01 | 2.59E-01 |
| $f_3$ | Best | 2.50E-01 | 5.39E-01 | 9.09E-07 |
| | Std. | 6.85E+02 | 9.61E-05 | 1.65E-01 |
| $f_4$ | Best | -1.13E+04 | -1.97E+01 | -8.38E+02 |
| | Std. | 1.47E+03 | 3.68E-01 | 3.56E+00 |
| $f_5$ | Best | 0.00E+00 | 0.00E+00 | 0.00E+00 |
| | Std. | 9.66E+00 | 7.30E-04 | 5.28E-03 |
| $f_6$ | Best | 6.22E-01 | 5.40E-02 | 1.10E-02 |
| | Std. | 1.93E+05 | 1.28E-03 | 2.55E-02 |

These statistical tests highlight the significant differences, consistency, and accuracy of the proposed algorithm. Based on the outcomes, it is clear that HHOA outperforms the CSA and BA methods, demonstrating superior exploration and exploitation capabilities, along with improved consistency and accuracy.

The process of finding the optimal solution using the algorithm is illustrated through convergence curves, which track the progression of the best solution at each iteration. Fig. 5 displays the normalized average convergence curves of the evaluated algorithms over 30 runs for both unimodal and multimodal benchmark functions. These curves offer insights into the performance and effectiveness of each algorithm in reaching optimal solutions. It is clear that HHOA demonstrates a superior convergence curve compared to CSA and BA, converging more quickly to the optimal solution and showing a stronger ability to avoid local optima. These results underscore the advantages of the HHOA-based approach for solving optimization problems, particularly in the context of SLTF.

### 4.2 Load forecasting optimization

The first step is to determine the set and constraints of the fuzzy logic MF parameters optimized using CSA, BA, and HHOA. Table 6 presents the parameters and constraints of the IT1FL MF optimized using these methods, while Table 7 provides the parameters and constraints of the IT2FL MF optimized similarly. The short-term load forecasting (STLF) model is designed for January 4, 2016, using input data from the same date over the previous six years.

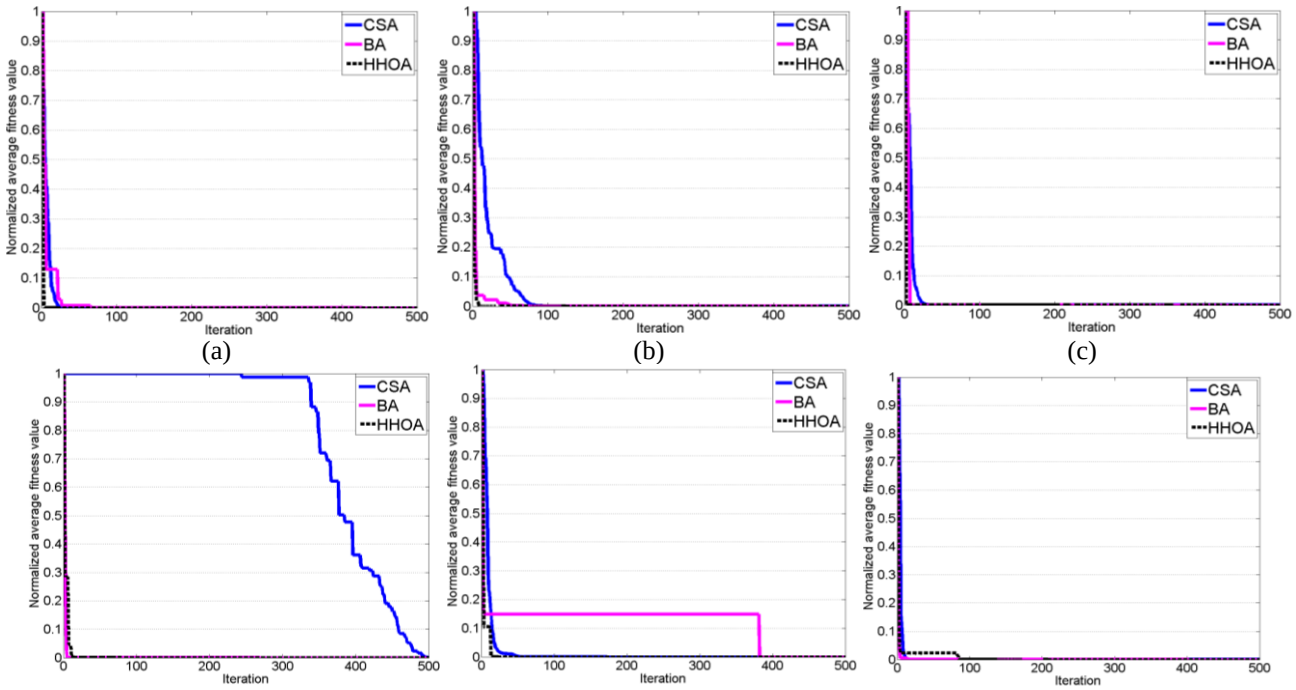


Figure. 5 The comparison of the convergence curve of the algorithms in unimodal and multimodal benchmark functions: (a) $f_1$, (b) $f_2$, (c) $f_3$, (d) $f_4$, (e) $f_5$, and (d) $f_6$

Table 6. IT1FL MF set

| MF | Set | Limitation |
|---|---|---|
| 1 | [175 ***200*** 225] | 195-205 |
| 2 | [200 ***225*** 250] | 220-230 |
| 3 | [225 ***250*** 275] | 245-255 |
| 4 | [250 ***275*** 300] | 270-280 |
| 5 | [275 ***300*** 325] | 295-305 |
| 6 | [300 ***325*** 350] | 320-330 |
| 7 | [325 ***350*** 375] | 345-355 |
| 8 | [350 ***375*** 400] | 370-380 |
| 9 | [375 ***400*** 425] | 395-405 |
| 10 | [400 ***425*** 450] | 420-430 |
| 11 | [425 ***450*** 475] | 445-455 |
| 12 | [450 ***475*** 500] | 470-480 |
| 13 | [475 ***500*** 525] | 495-505 |
| 14 | [500 ***525*** 550] | 520-530 |
| 15 | [525 ***550*** 575] | 545-555 |
| 16 | [550 ***575*** 600] | 570-580 |
| 17 | [575 ***600*** 625] | 595-605 |
| 18 | [600 ***625*** 650] | 620-630 |
| 19 | [625 ***650*** 675] | 645-655 |
| 20 | [650 ***675*** 700] | 670-680 |
| 21 | [675 ***700*** 725] | 695-705 |
| 22 | [700 ***725*** 750] | 720-730 |
| . | . | . |
| . | . | . |
| . | . | . |
| 29 | [875 ***900*** 925] | 895-905 |
| 30 | [900 ***925*** 950] | 920-930 |
| 31 | [925 ***950*** 975] | 945-955 |
| 32 | [950 ***975*** 1000] | 970-980 |
| 33 | [975 ***1000*** 1025] | 995-1005 |

Table 7. IT2FL MF set

| MF | Set | Limitation |
|---|---|---|
| 1 | [175 200 ***215 185*** 205 225] | 210-220,180-190 |
| 2 | [200 225 ***240 210*** 230 250] | 235-245,205-215 |
| 3 | [225 250 ***265 235*** 255 275] | 260-270,230-240 |
| 4 | [250 275 ***290 260*** 280 300] | 285-295,255-265 |
| 5 | [275 300 ***315 285*** 305 325] | 310-320,280-290 |
| 6 | [300 325 ***340 310*** 330 350] | 335-345,305-315 |
| 7 | [325 350 ***365 335*** 355 375] | 360-370,330-340 |
| 8 | [350 375 ***390 360*** 380 400] | 385-395,355-365 |
| 9 | [375 400 ***415 385*** 405 425] | 410-420,380-390 |
| 10 | [400 425 ***440 410*** 430 450] | 435-445,405-415 |
| 11 | [425 450 ***465 435*** 455 475] | 460-470,430-440 |
| 12 | [450 475 ***490 460*** 480 500] | 485-495,455-465 |
| 13 | [475 500 ***515 485*** 505 525] | 510-520,480-490 |
| 14 | [500 525 ***540 510*** 530 550] | 535-545,505-515 |
| 15 | [525 550 ***565 535*** 555 575] | 560-570,530-540 |
| 16 | [550 575 ***590 560*** 580 600] | 585-595,555-565 |
| 17 | [575 600 ***615 585*** 605 625] | 610-620,580-590 |
| 18 | [600 625 ***640 610*** 630 650] | 635-645,605-615 |
| 19 | [625 650 ***665 635*** 655 675] | 660-670,630-640 |
| 20 | [650 675 ***690 660*** 680 700] | 685-695,655-665 |
| 21 | [675 700 ***715 685*** 705 725] | 710-720,680-690 |
| 22 | [700 725 ***740 710*** 730 750] | 735-745,705-715 |
| . | . | . |
| . | . | . |
| . | . | . |
| 29 | [875 900 ***915 885*** 905 925] | 910-920,880-890 |
| 30 | [900 925 ***940 910*** 930 950] | 935-945,905-915 |
| 31 | [925 950 ***965 935*** 955 975] | 960-970,930-940 |
| 32 | [950 975 ***990 960*** 980 $10^3$] | 985-995,955-965 |
| 33 | [975 1000 ***1015 985*** 1005 1025] | 1010-1020,980-990 |

The optimization of the FOU in IT2FL using HHOA for is performed through an m-file program in MATLAB, utilizing functions from the IT2FL Toolbox to obtain the forecast values. The forecast results are then processed in MS Excel to derive peak load forecasts and calculate forecast errors. A comparison of the forecasting results and STLF errors using the IT2FL-CSA, IT2FL-BA, and the proposed IT2FL-HHOA methods for 2016 is presented in Figs. 6 and 7. Additionally, load forecasting results using the IT1FL-CSA, IT1FL-BA, and IT1FL-HHOA methods are included for further comparison.

The results of the STLF optimization using the proposed IT2FL-HHOA method yielded a minimum MAPE of 1.5567%, while the IT2FL-CSA method produced a MAPE of 1.6289%, and the IT2FL-BA method produced a MAPE of 1.6386%. In comparison, the IT1FL-HHOA method achieved a MAPE of 1.6604%, the IT1FL-CSA method resulted in a MAPE of 1.6737%, and the IT1FL-BA method resulted in a MAPE of 1.6704%.

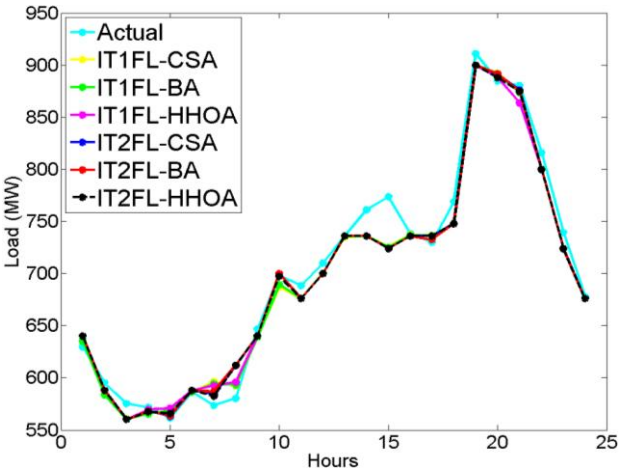


Figure. 6 Comparison of STLF results

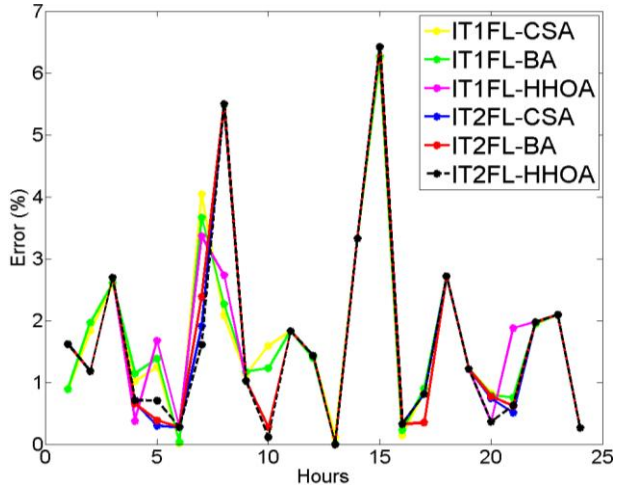


Figure. 7 Comparison of error STLF results

This study proposes the application of the HHOA swarm intelligence optimization method for optimizing the FOU in fuzzy logic within the STLF system of Sulbagsel. HHOA operates based on an objective function to minimize the MAPE value. Through benchmark testing and implementation in STLF, this study demonstrates that the HHOA method outperforms the CSA and BA methods. HHOA shows superior exploration and exploitation capabilities, along with improved consistency and accuracy in determining the appropriate FOU parameters, leading to optimal STLF outcomes.

## 5. Conclusion

This paper introduces a novel swarm intelligence technique, the Horse Herding Optimization Algorithm (HHOA), inspired by the social behavior of horses of different ages. The algorithm incorporates six significant traits: grazing, hierarchy, sociability, imitation, defense mechanisms, and roaming. These traits are aimed at optimizing the footprint of uncertainty (FOU) in interval type-2 fuzzy logic (IT2FL) for short-term peak load forecasting (STLF) within the Southern Sulawesi (Sulbagsel) system in Indonesia.

To evaluate the initial performance of HHOA, six benchmark functions were used to assess its exploration, exploitation, ability to avoid local optima, and convergence. The results indicate that HHOA is highly competitive with other swarm intelligence methods, such as the Cuckoo Search Algorithm (CSA) and Bat Algorithm (BA). Specifically, HHOA demonstrates superior exploitation on unimodal functions and improved exploration on multimodal functions.

The optimization of the FOU in IT2FL using the HHOA for STLF in the Sulbagsel system shows that the mean absolute percentage error (MAPE) for the IT2FL-HHOA method is 1.5567%, which is lower than that of the other methods. In comparison, the MAPE for the IT2FL-CSA method is 1.6289%, and for the IT2FL-BA method, it is 1.6386%. The MAPE values for IT1FL-HHOA, IT1FL-CSA, and IT1FL-BA are 1.6604%, 1.6737%, and 1.6704%, respectively. All MAPE values remain below the allowable tolerance limit.

## Acknowledgments

This research was funded by the Directorate of Research and Community Service, Universitas Hasanuddin, Makassar, Indonesia, through the 2024 Indonesian Collaborative Research Program (RKI), under contract number 01369/UN4.22/PT.01.03/2024.

## Conflicts of Interest

The authors declare no conflict of interest.

## Author Contributions

Conceptualization, S, MRD; Methodology, HRG, VL; Software, MRD, MAP, WH; Validation, IR, S, RNH; Formal Analysis, MRD, MAP; Investigation, RNH, MRD; Resources: HLG, VL, WH; Writing Original Draft Preparation, MRD; Writing Review and Editing, MAP; Visualization, MRD.

**Notation List**

| Parameters | Notation |
|---|---|
| $\widetilde{\boldsymbol{A}}$ | IT2FL |
| $\mu\tilde{A}$ | IT2FL Membership Function |
| $Jx$ | Primary membership function |
| $\underline{\mu}\tilde{A}$ | Lower membership function |
| $\bar{\mu}\tilde{A}$ | Upper membership function |
| X1-X6 | Load Data |
| Z1 | Forecast of the predicted day |
| Delta (δ) | Horses aged 0 to 5 years |
| Gamma (γ) | Horses aged 5 to 10 years |
| Beta (β) | Horses aged 10 to 15 years |
| Alpha (α) | Horses older than 15 years |
| $\overline{V}_k^{Age,Itr}$ | Age range and velocity vector of the horse |
| $Itr$ | Iteration |
| $X$ | Average position of the best horses |
| pN | Number of horses with the best location |
| $S_i^{Iter,Age}$ | Social movement vector of horse $i$ |
| $N$ | Total number of horses |
| $D_i^{Iter,Age}$ | Escape vector of the $i_{th}$ horse |
| $qN$ | Horse with the worst possible location |
| $q$ | Total number of horses. |
| $R_i^{Iter,Age}$ | Random velocity vector |

## References


[1] M. Short, T. Crosbie, M. Dawood, and N. Dawood, "Load forecasting and dispatch optimisation for decentralised co-generation plant with dual energy storage", *Applied Energy*, Vol. 186, pp. 304-320, 2017.

[2] A. Al Mamun, M. Sohel, N. Mohammad, M. S. H. Sunny, D. R. Dipta, and E. Hossain, "A comprehensive review of the load forecasting techniques using single and hybrid predictive models", *IEEE access*, Vol. 8, pp. 134911-134939, 2020.

[3] H. Habbak, M. Mahmoud, K. Metwally, M. Fouda, and M. Ibrahem, "Load Forecasting Techniques and Their Applications in Smart Grids", *Energies*, Vol. 16, p. 1480, 2023.

[4] H. Wang, K. A. Alattas, A. Mohammadzadeh, M. H. Sabzalian, A. A. Aly, and A. Mosavi, "Comprehensive review of load forecasting with emphasis on intelligent computing approaches", *Energy Reports*, Vol. 8, pp. 13189-13198, 2022.

[5] S. Haleema, "Short-Term Load Forecasting using Statistical Methods: A Case Study on Load Data", *International Journal of Engineering Research and*, Vol. V9, 2020.

[6] Y.-Y. Hong and Y.-H. Chan, "Short-term electric load forecasting using particle swarm optimization-based convolutional neural network", *Engineering Applications of Artificial Intelligence*, Vol. 126, p. 106773, 2023.

[7] P. Bento, J. Pombo, S. Mariano, and M. d. R. Calado, "Short-Term Load Forecasting using optimized LSTM Networks via Improved Bat Algorithm", In: *Proc. of 2018 International Conf on Intelligent Systems (IS)*, pp. 25-27 pp. 351-357, 2018.

[8] L. I. U. H, S. U. N. X, X. U. L, G. U. S, and S. U. N. F, "Short-term load forecasting based on Elman Neural Network optimized by Firefly Algorithm", In: *Proc. of 2019 IEEE Innovative Smart Grid Technologies - Asia (ISGT Asia)*, pp. 1425-1429, 2019.

[9] S. K. Panda, P. Ray, D. P. Mishra, and S. R. Salkuti, "Short-term load forecasting of the distribution system using cuckoo search algorithm", *International Journal of Power Electronics and Drive Systems*, Vol. 13, No. 1, pp. 159-166, 2022.

[10] Z. Cai, S. Dai, Q. Ding, J. Zhang, D. Xu, and Y. Li, "Gray wolf optimization-based wind power load mid-long term forecasting algorithm", *Computers and Electrical Engineering*, Vol. 109, p. 108769, 2023.

[11] T. Hu, M. Zhou, K. Bian, W. Lai, and Z. Zhu, "Short-Term Load Probabilistic Forecasting Based on Improved Complete Ensemble Empirical Mode Decomposition with Adaptive Noise Reconstruction and Salp Swarm Algorithm", *Energies*, Vol. 15, No. 1, p. 147, 2022.

[12] B. Li, H. Sun, and M. Teimourian, "Optimal electric load forecasting for systems by an adaptive Crow Search Algorithm: A case study", *Concurrency and Computation: Practice and Experience*, Vol. 34, No. 21, p. e7120, 2022.

[13] A. Ramadhani, I. Robandi, M. R. Djalal, and M. A. Prakasa, "Modeling of Power Management Systems for Healtcare Facilities Using Hybrid

Fuzzy-Particle Swarm Optimization: A Case Study of Ulin Hospital", In: *Proc. of 2024 International Seminar on Intelligent Technology and Its Applications*, pp. 424-429, 2024.

[14] A. K. De, D. Chakraborty, and A. Biswas, "Literature review on type-2 fuzzy set theory", *Soft Computing*, Vol. 26, No. 18, pp. 9049-9068, 2022.

[15] N. N. Karnik and J. M. Mendel, "Introduction to type-2 fuzzy logic systems", In: *Proc. of 1998 IEEE International Conf on Fuzzy Systems Proceedings. IEEE World Congress on Computational Intelligence*, Vol. 2, pp. 915-920, 1998.

[16] I. Robandi and I. Anshory, "A very short-term load forecasting in time of peak loads using interval type-2 fuzzy inference system: A case study on java bali electrical system", *Journal of Engineering Science And Technology*, Vol. 14, No. 1, pp. 464-478, 2019.

[17] W. Zou, C. Li, and P. Chen, "An Inter Type-2 FCR Algorithm Based T–S Fuzzy Model for Short-Term Wind Power Interval Prediction", *IEEE Transactions on Industrial Informatics*, Vol. 15, No. 9, pp. 4934-4943, 2019.

[18] E. N. Moyo, G. Sharma, P. N. Bokoro, V. Rameshar, and L. Muremi, "Short-Term Load Forecasting Using Application of Interval Type 2 Fuzzy Logic", In: *Proc. of 2024 32nd Southern African Universities Power Engineering Conference*, pp. 1-6, 2024.

[19] H. Mo, F. Y. Wang, M. Zhou, R. Li, and Z. Xiao, "Footprint of uncertainty for type-2 fuzzy sets", *Information Sciences*, Vol. 272, pp. 96-110, 2014.

[20] F. P. Nishanth, S. K. Dash, and S. R. Mahapatro, "Critical study of type-2 fuzzy logic control from theory to applications: A state-of-the-art comprehensive survey", *e-Prime - Advances in Electrical Engineering, Electronics and Energy*, Vol. 10, p. 100771, 2024.

[21] F. MiarNaeimi, G. Azizyan, and M. Rashki, "Horse herd optimization algorithm: A nature-inspired algorithm for high-dimensional optimization problems", *Knowledge-Based Systems*, Vol. 213, p. 106711, 2021.

[22] S. Sarwar, M. A. Hafeez, M. Y. Javed, A. B. Asghar, and K. Ejsmont, "A Horse Herd Optimization Algorithm (HOA)-Based MPPT Technique under Partial and Complex Partial Shading Conditions", *Energies*, Vol. 15, No. 5, p. 1880, 2022.

[23] M. A. Awadallah, A. I. Hammouri, M. A. Al-Betar, M. S. Braik, and M. Abd Elaziz, "Binary Horse herd optimization algorithm with crossover operators for feature selection", *Computers in Biology and Medicine*, Vol. 141, p. 105152, 2022,

[24] G. Lin, B. Qi, C. Ma, and F. Rostam, "Intelligent electric vehicle charging optimization and horse herd-inspired power generation for enhanced energy management", *Energy*, Vol. 291, p. 130395, 2024.

[25] R. Abbassi and S. Saidi, "Design of a Novel Chaotic Horse Herd Optimizer and Application to MPPT for Optimal Performance of Stand-Alone Solar PV Water Pumping Systems", *Mathematics*, Vol. 12, No. 4, p. 594, 2024.

[26] A. Refaat *et al.*, "Extraction of maximum power from PV system based on horse herd optimization MPPT technique under various weather conditions", *Renewable Energy*, Vol. 220, p. 119718, 2024.

[27] A. RamaKrishnan, A. Shunmugalatha, and K. Premkumar, "An Improved Tuning of PID Controller for PV Battery-Powered Brushless DC Motor Speed Regulation Using Hybrid Horse Herd Particle Swarm Optimization", *International Journal of Photoenergy*, Vol. 2023, No. 1, p. 2777505, 2023.

[28] M. Saini, M. R. Djalal, and A. Yunus, "Design of a Robust PID-PSS & FACTS Using Craziness Particle Swarm Optimization in Sulselrabar System", *International Journal of Intelligent Engineering & Systems*, Vol. 17, No. 4, 2024, doi: 10.22266/ijies2024.0831.38.

[29] I. Robandi, M. R. Djalal, and M. A. Prakasa, "Performance Improvement of Sulselrabar System Using Single-Band Power System Stabilizer Based on Mayfly Algorithm Under Different Loading Condition", *International Journal of Intelligent Engineering & Systems*, Vol. 17, No. 1, pp. 370-382, 2024, doi: 10.22266/ijies2024.0229.33.

[30] I. Robandi, M. R. Djalal, and M. A. Prakasa, "Performance Improvement of Sulselrabar System Using Single-Band Power System Stabilizer Based on Mayfly Algorithm Under Different Loading Condition", *International Journal of Intelligent Engineering & Systems*, Vol. 17, No. 1, 2024, doi: 10.22266/ijies2024.0229.33.

[31] M. R. Djalal, I. Robandi, and M. A. Prakasa, "Stability Improvement of Sulselrabar System With Integrated Wind Power Plant Using Multi-Band PSS3C Based Mayfly Optimization Algorithm", *IEEE Access*, Vol. 12, pp. 76707-76734, 2024.